UDC 621.371
doi:10.31799/1684-8853-2019-6-43-53

Articles

Analysis of total signal decay and capacity of information data in wireless atmospheric communication links. Part 1

Juwiler I.[a], *PhD, Senior Lecturer, orcid.org/0000-0002-0669-7828*
Bronfman I.[a], *Assistant, orcid.org/0000-0001-6195-069X*
Blaunstein N.[b], *Dr. Sc., Phys.-Math., Professor, orcid.org/0000-0003-2945-9379, nathan.blaunstein@hotmail.com*
[a]*Electrical and Electronics Engineering Department, Shamoon College of Engineering, Jabotinsky St., 84, Ashdod, 77245, Israel*
[b]*Ben-Gurion University of the Negev, P.O.B. 653, 1, Ben-Gurion St., Beer-Sheva, 74105, Israel*

Introduction: *Analysis of total signal decay is based on prognosis of the total path loss occurring in the atmospheric communication links, accounting for effects of gaseous structures attenuation and scattering, hydrometeors (rain, snow and clouds) absorption and attenuation, and turbulent structures fast fading on radio and optical signals passing atmospheric channels with fading.* ***Purpose:*** *To perform a novel methodology of definition and estimation of effects of decay, absorption, scattering, and fading of radio and optical signals propagating in atmospheric channels in various meteorological conditions.* ***Results:*** *Was analyzed the impact of gaseous structures, hydrometeors and turbulent structures in total path loss for link budget design and in degradation of data stream parameters, such as capacity, spectral efficiency and bit-error-rate, which lead in loss of information data signals passing such kinds of channels with fast fading and decrease of quality of service. An optimal algorithm was found of the total path loss prediction for various meteorological situations occurring in the real atmosphere at different heights and for various frequencies of radiated signals. A method was proposed of how to evaluate the data stream parameters, capacity, spectral efficiency and bit-error-rate, accounting for the effects of atmospheric turbulence impact on fast fading, which corrupts information passing such kinds of channels. All practical tests were illustrated by the use of the MATLAB utility. A new methodology was proposed on how to evaluate and estimate the capacity, the spectral efficiency, and the loss in energy and in the information data stream for different scenarios of radio and optical signals propagation via atmospheric channels with fading caused by different meteorological conditions.* ***Practical relevance:*** *The results obtained allow to achieve better accuracy of prognosis and increase quality of service in atmospheric communication channels.*

Keywords *— absorption, attenuation, bit-error rate, capacity, clouds, fast fading, gaseous structures, hydrometeors, rain, Ricean factor K, snow, scintillation index, spectral efficiency, turbulence.*

For citation: Juwiler I., Bronfman I., Blaunstein N. Analysis of total signal decay and capacity of information data in wireless atmospheric communication links. Part 1. *Informatsionno-upravliaiushchie sistemy* [Information and Control Systems], 2019, no. 6, pp. 43–53. doi:10.31799/1684-8853-2019-6-43-53

Overview

There are three main channels of wireless communications: the terrestrial, atmospheric and ionospheric. In this work, we will discuss the atmospheric channel, mainly the tropospheric one, which is the lower region of the atmosphere that surrounds the Earth from the ground surface up to 10–20 km above the terrain (Fig. 1). During the recent decades (see [1–7] and bibliography therein) the most attractive aspect for current investigations has become the land-to-air and air-to-land communication links with aircrafts such as airplanes, helicopters, drones, and so forth. As follows from Fig. 1, the troposphere consists of gaseous particles, called aerosols, rain particles, clouds, fog, hail, snow, and so on, all of which are usually called hydrometeors in the literature [8–19]. Furthermore, due to sporadic air streams and motions, another phenomenon occurs in the troposphere called atmospheric turbulences. Due to irregular conditions in the troposphere, when a radio or optical signal propagates through a tropospheric channel, its intensity varies sporadically. This phenomenon is called fading, fast and slow in the time domain, or small-scale and large-scale in the space domain, respectively [3–5].

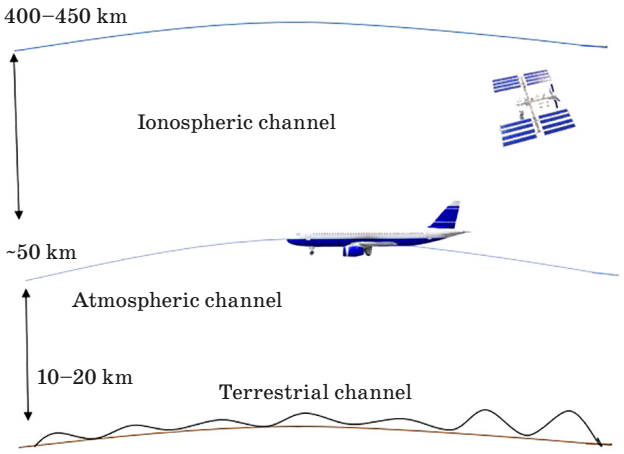

■ ***Fig. 1.*** Main communication links

The aim of the work under our recent investigations is to design a link budget, that is, to evaluate the total signal path loss via prediction of the effects of main tropospheric features on propagation of signals with data through such channels. At the same time — to perform quality of service within the atmospheric link by estimating parameters of signal data stream passing atmospheric wireless channels, with fading caused by multiple scattering, reflection and diffraction of radio waves as the carrier of information. Finally, the aim of this work is to provide designers of wireless atmospheric communication links a stable algorithm of how to:

— predict the total path loss;

— design a link budget;

— perform and improve quality of service by predicting a-priori the capacity of data stream or spectral efficiency and bit-error-rate (BER) in such channels affected by attenuation, absorption and fading phenomena.

Content and main parameters of the troposphere

The troposphere consists of different kinds of gaseous, liquid and crystal structures such as gas molecules, aerosol, rain particles, cloud, fog, hail and snow. All except the first, are usually called *hydrometeors* in the literature. Furthermore, due to sporadic air streams and motions another phenomenon occurs in space and time domains, called atmospheric turbulences. Below, we briefly describe the various components that make up the troposphere following the specific literature [1–3, 8–22].

The content

Gaseous molecules and atoms. There are many types of atmospheric molecules and atoms, such as O_2, O, CO_2, NO, N_2, etc. [1–3, 20].

An aerosol, for the purposes of this paper, is a system of liquid or solid particles uniformly dispersed in the atmosphere. Aerosol particles play an important role in the perception process, providing the nuclei upon which condensation and freezing take place. The particles participate in chemical processes and influence the electrical properties of the atmosphere [18, 19]. The system begins to acquire the properties of a real aerosol structure when smaller particles are in suspension. An actual aerosol particle range can be between a few nanometers to about few micrometers, while aerosols composed of particles larger than 50 μm are unstable. The number of aerosol molecules can be found [19]:

$$N(z) = N(0)\exp\left(\frac{z}{z_s}\right), \qquad (1)$$

where $N(z)$ is the current number of molecules; $N(0)$ is the number of molecules at the ground surface; z is the height of the molecules in meters, and z_s is scale height while 1 km $< z_s <$ 1.4 km.

Clouds. Clouds' shape, structure and texture are influenced by air movements that change their formation and growth, and are also influenced by the properties of the cloud particles themselves. There are four principle classes into which clouds are classified according to the kind of air motions that produce them [2, 11–13]:

1) layer clouds formed by the widespread regular ascent of air;

2) layer clouds formed by the widespread irregular stirring of turbulence;

3) cumuliform clouds formed by penetrative convection;

4) orographic clouds formed by ascent of air over hills and mountains.

In settled weather, clouds are small and well scattered. Their horizontal and vertical dimensions are only a kilometer or two. In disturbed weather, they cover a large part of the sky and can tower as high as 10 km or more. Clouds often cease their growth only upon reaching the stable stratosphere, producing heavy showers, hail, and thunderstorms. Growing clouds are sustained by upward air currents, which may vary in strength from a few centimeters per second to several meters per second. Cloud effects on wave propagation in the troposphere are well known. These effects are scattering, absorption and refraction which all cause attenuation and fading of the wave path. All these phenomena will be considered later.

Rain is the precipitation of liquid water drops with diameters greater than 0.5 mm [14–17]. When the drops are smaller, the precipitation is usually called drizzle. The concentration of raindrops typically spreads from 100 to 1000 m^{-3}. Drizzle droplets usually are more numerous. Raindrops seldom have diameters larger than 4 mm because the concentration generally decreases as the diameter increases, except when the rain is heavy. It does not reduce visibility as much as drizzle. Meteorologists classify rain according to its rate of fall. There are three classes of rain: light, moderate and heavy and they correspond to dimensions less than 2.5 mm, between 2.8 and 7.6 mm, and more than 7.6 mm, respectively. As for rain with rates of less than 250 mm per year and for more than 1500 mm per year, that represents the extremes of rainfall for all the continents.

Atmospheric turbulence is a chaotic structure generated by irregular air movements in which the wind randomly varies in speed and direction [5–7, 23–26]. Turbulence is important because it churns and mixes the atmosphere and causes water vapor, smoke, and other substances, as well as energy, to

become distributed at all elevations. Atmospheric turbulence near the Earth's surface differs from that which occurs at higher levels. Within a few hundred meters of the surface, turbulence has a marked diurnal variation, reaching a maximum about midday. When the sky is cloudy, the low-level air temperature varies much less between day and night and turbulence remains nearly constant. At altitudes of several thousand meters or more, the frictional effect of the Earth's surface topography on the wind is greatly reduced and the small-scale turbulence, which is usually observed in the lower atmosphere, is absent [4–7].

Main parameters of troposphere

The physical properties of the troposphere are characterized by the following main parameters such as *temperature*, T (in Kelvin), *pressure*, P (in millibar or millimeters of Mercury), and *density*, p (in particles per cubic meter or centimeter). All these parameters significantly change with altitude, seasonal, and latitudinal variability, and strongly depend on the weather [3].

Temperature. The temperature in the atmosphere depends on altitude h, in meters. The temperature T at height h (measured in meters) is given by [4–7]:

$$T(h) = 288.15 + 0.06545h \text{ K} \quad (2)$$

the troposphere is a region between 10–20 km above the earth's surface, and in this region the temperature is [4–7]:

$$T(h) = 216.65 \text{ K}. \quad (3)$$

Pressure. It is the force-applied perpendicular to the surface of an object per unit area over which that force is distributed. The pressure can be determined by [4–7]:

$$P(h) = 2.269 \times$$
$$\times 10^4 \exp\left[-\frac{0.034164(h-11\,000)}{216.65}\right] \text{mbar}, \quad (4)$$

where h is the height (in meters). In the troposphere, besides the atmospheric pressure, we usually need to know the water vapor partial pressure p, [mbar], and $e(t)$ is the saturation pressure [6]. The relationship between water vapor pressure p_w and relative humidity is given by:

$$\rho_w = \frac{\eta e_s}{100}, \quad (5)$$

where

$$e_s = a\frac{bt}{t+c}, \quad (6)$$

where η is the relative humidity, %; t is the temperature, °C; e_s is the saturation pressure, Pa, for temperature t, °C, while the coefficients a, b, and c were defined empirically via numerous experiments [6]. The vapor pressure p can be evaluated via the water vapor density ρ using the equation

$$p_w = \frac{\rho_w T(h)}{216.7} \quad (7)$$

with the water vapor density ρ given by the following equation:

$$\rho = \rho_0 \exp\left(-\frac{h}{h_0}\right). \quad (8)$$

Here, h_0 is the scale height of 2 km and the standard water vapor density is:

$$\rho_0 = 7.5 \ \frac{\text{g}}{\text{m}^{-3}}. \quad (9)$$

Humidity. In meteorology the measurable quantity is the relative humidity $\eta(T)$, and we can relate p with $e_s(T)$. The relative humidity is given by [4–6]:

$$\eta = \frac{\rho_w}{e_s(T)}. \quad (10)$$

Effects of tropospheric features on signal propagation

For the ideal fully gaseous atmosphere with an absence of hydrometeors, fading phenomena of radio and optical waves can remain optimal 99.999 % of the time for the paths of 5 km and more, with the fade margin of 28 dB. However, there are phenomena of propagation that can significantly decrease the efficiency of land-to-atmosphere or atmosphere-to-land communication links, such as scattering, attenuation or absorption. Let us briefly consider the impact of each feature separately in total path loss of the signal passing a tropospheric communication channel.

Main features occurring in the troposphere

Absorption (or ***attenuation***) occurs because of conversion from wave energy to thermal energy within an attenuating particle, such as a gas molecule and different hydrometeors [3–5].

Scattering is a vitally important feature causing strong fast fading of the signal and occurs from the redirection of the radio waves into various directions, so that only a fraction of the incident energy is transmitted onward in the direction of the receiver. The main scattering particles that are of

interest to satellite systems are hydrometeors, including raindrops, fog and clouds; and can be calculated using three main approaches that account for the relationship between the wavelength and the size of the particles causing the scatter. All approaches were discussed in [3–7, 23] and their scattering coefficient is described below by the following theoretical frameworks (11a)–(11c).

a) *Mie scattering* is applicable when the particle size is comparable to the radiation wavelength. The Mia scattering coefficient was defined as the ratio of the incident wave front that is affected by the particle to the cross-sectional:

$$\sigma_\lambda = \pi \int_{a_1}^{a_2} N(r) K(r, n) r^2 \, \mathrm{d}r. \qquad (11a)$$

b) *Rayleigh scattering* applies when the radiation wavelength is much smaller than the particle sizes and is described by

$$\sigma_\lambda = \frac{\left(\frac{4\pi^2 N V^2}{\lambda^2}\right)\left(n^2 - n_0^2\right)^2}{\left(n^2 + 2n_0^2\right)^2}, \qquad (11b)$$

where n_0 an index of refraction at the ground level.

c) *Non-selective scattering* applies when the particle size is significantly larger than the radiation wavelength. Large-particle scattering is composed of contributions from three processes involved in the interaction of the electromagnetic radiation with the scattering particles:

$$\sigma_\lambda = \int N(r) Q(\lambda, m, r) \pi r^2 \, \mathrm{d}r. \qquad (11c)$$

Here N is a number of particles per unit volume; r is the radius of spherical particle; K is a value between 0 to 4; n is an index of the refraction of waves at the layer of particles; V is the volume of scattering particles, and m is the mass of any particle.

The above formulas account for the following physical processes caused by gaseous particles of the troposphere:

— reflection from the surface of the particle with no penetration;

— passage through the particle with and without internal reflection;

— diffraction at the edge of the particle.

Effects of tropospheric features on signal passing the channel

Now, we will examine separately the effects of each feature on signals passing the irregular troposphere, such as the effects of rain and cloud on the signal attenuation. The effect of turbulence causing scattering of signals will be considered separately as a main source of fast fading. There are three main causes for signal attenuations: molecular absorption, effects of rain and effect of clouds. Then the effect of turbulence on scattering of signals will be presented. We will show the main parameters, the corresponding formulas, and will compute and plot their characteristics in this paragraph.

Molecular-gaseous absorption

Gaseous molecules found in the atmosphere may absorb energy from radio-waves passing through them, thereby causing attenuation [1–3, 20]. The signal degradation depends on frequency, temperature, pressure, and water vapor concentration; and increases with them as shown in Fig. 2 calculated according to the equations below taken from ITU-676 Standard [20] for pressure $P = 1013$ mbar, temperature $T = 15$ °C, water vapor content $\rho_w = 7.5$ g/m^{-3}. The following formulas have been used for computation of dependences shown in Fig. 2.

The absorption in the atmosphere over path length r is given by [20]:

$$A = \int \gamma(r) \mathrm{d}r, \qquad (12)$$

where $\gamma(r)$ is specific attenuation, dB/km, consisting of the sum of two components $\gamma_o(r)$ and $\gamma_w(r)$, the attenuation of oxygen and water vapor, respectively:

$$\gamma(r) = \gamma_o(r) + \gamma_w(r), \qquad (13)$$

$\gamma_o(r)$ and $\gamma_w(r)$ at the ground level (where pressure is 1013 mbar and temperature is 15 °C), are given approximately by [20]:

$$\gamma_o = \left[7.19 \times 10^{-3} + \frac{6.09}{f^2 + 0.227} + \frac{4.81}{(f-57)^2 + 1.5}\right] \times f^2 \times 10^{-3} \left[\frac{\mathrm{dB}}{\mathrm{km}}\right]; \qquad (14)$$

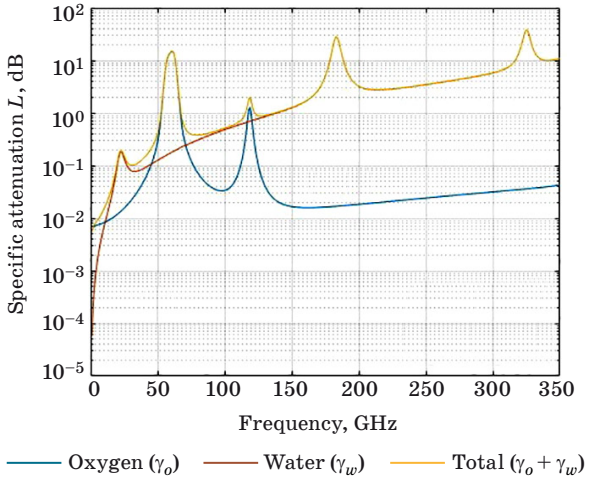

■ ***Fig. 2.*** Specific attenuation for water vapor and oxygen (pressure = 1013 mbar, temperature = 15 °C, water vapor content = 7.5 g/m^{-3})

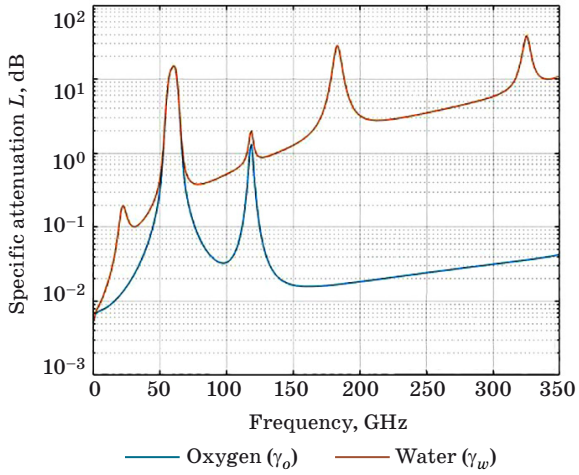

■ ***Fig. 3.*** The total zenith attenuation versus frequency for gaseous atmosphere with water vapor and dry air

$$\gamma_w = \left[0.05 + 0.0021\rho + \frac{6.09}{(f-22.2)^2 + 8.5} + \frac{10.6}{(f-18.3)^2 + 9} \right] f^2 \rho \times 10^{-4} \left[\frac{\text{dB}}{\text{km}} \right], \quad (15)$$

where f is the frequency, GHz, and ρ is the water vapor density, g/m^{-3}.

Other temperatures are considered by correction factors of −1,0 % per 1 °C from 15 °C for dry air, and −0,6 % per 1 °C from 15 °C for water vapor.

The attenuation in the atmosphere over a path length L, for oxygen, L_o, and for water vapor, L_w, is given by [20]:

$$A_o = \gamma_o L_o; A_w = \gamma_w L_w \text{ [dB]}. \quad (16)$$

The total atmospheric attenuation [in dB] for a particular path can then be found by integrating the total specific attenuation, as shown in Fig. 3, over the total path length in the atmosphere [20] by assuming an exponential decrease in gas density with height:

$$L_a = \int_0^{\pi} \gamma_a(l)\,\mathrm{d}l = \int_0^{\pi} \left[\gamma_o(l) + \gamma_w(l) \right] \mathrm{d}l. \quad (17)$$

The attenuation for an inclined path with an elevation angle $\theta > 10°$ can then be found from the zenith attenuation L_z as [3, 20]

$$L_a = \frac{L_z}{\sin\theta} \quad (18)$$

and was computed by equations (13)–(18) following the parameters of the troposphere according to the standard ITU-676 [20].

Effects of rain

The attenuation of radio waves caused by rain increases with the number of raindrops along the radio path, the size of the drops, and the length of the path through which the rain passes as shown in Fig. 4 rearranged from [3].

There are several models for finding the attenuation caused by rain: Empirical [15], Semi-Empirical [14, 16], and Statistical-Analytical Models, such as Saunders's model [3]. The Saunders's model which was embraced by ITU, does not depend on a particular place, is not frequency dependent, has a good processing time, and can be easily implemented.

In our work we followed only the Saunders's model. The Saunders's model is applied when the density and shape of the raindrops are constant. According to [3], the received power P_r in a given antenna is found to drop exponentially with radio path r through the rain, and α as the reciprocal of distance required for the power decreases to e^{-1} of its initial value:

$$P_r(r) = P_r(0)e^{-\alpha r}. \quad (19)$$

The value of α is given by the integral of one dimensional (1D) distribution of the drops diameter D, denoted by $N(D)$, and $C(D)$ is the effective cross-section of frequency dependent signal power attenuation by rain drops:

$$\alpha = \int_{D=0}^{\infty} N(D) \cdot C(D)\,\mathrm{d}D. \quad (20)$$

In a real tropospheric situation, the drop diameter distribution $N(D)$ is not a constant value and can be found by the next equation [3]:

$$N(D) = N_0 \exp\left(-\frac{D}{D_m} \right), \quad (21)$$

where N_0 and D_m are parameters: D_m is a parameter that depends on the rainfall rate remeasured

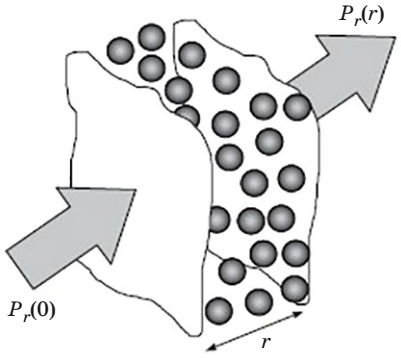

■ ***Fig. 4.*** Rain path attenuation

above the ground surface in millimeters per hour; $N_0 = 8 \times 10^3\ \mathrm{m^{-2}\,mm^{-1}}$, and

$$D_m = 0.122 \cdot r^{0.21}\ [\mathrm{mm}]. \quad (22)$$

As for $C(D)$ the attenuation cross-section from (20), can be found using *Rayleigh approximation* that is valid for lower frequencies, as was mentioned in [3], when the average drop size is smaller compared to the incident wavelength. In this case only absorption inside the drops occur and the Rayleigh approximation is valid giving a very simple expression for $C(D)$:

$$C(D) \propto \frac{D^3}{\lambda}. \quad (23)$$

As was mentioned in [3, 14–17], when $N(D)$ is not constant as we described earlier in (21) we take the value of the specific attenuation at a given point on the path, $\gamma(r)$, and integrate over the full path length R to find the total path loss:

$$L = \int_0^R \gamma(r)\,\mathrm{d}r, \quad (24)$$

while the total loss is via the specific attenuation as shown in [9] and defined by

$$\gamma = \frac{L}{r} 4.34\alpha. \quad (25)$$

Another way to describe the attenuation caused by rain is, when it increases more slowly with frequency approaching a constant value known as the *optical limit* [3]. Near this limit, scattering forms a significant part of attenuation that can be described using the *Mie* scattering theory that was described earlier [3, 4].

Expressing (25) in a logarithmic scale gives

$$L = 10\log\left(\frac{P_T}{P_R}\right) = 4.34\alpha r. \quad (26)$$

In practical situations, we can use an empirical model which implicitly combines all of these effects, where γ is assumed to depend only on distance r; whereas the rainfall rate (R) is measured on the ground in millimeters per hour. According to [3, 14–17]

$$\gamma(f, R) = a(f)R^{b(f)}. \quad (27)$$

The attenuation coefficients $a(f)$ and $b(f)$ can be found and calculated in [3, 15, 12]. The attenuation for a given path where the elevation angle θ is smaller than 90° makes it necessary to account for the variation in the rain in the horizontal direction. This allows us to focus on the finite size of rain clouds, called *rain cells*.

Also, rain varies in time over various parameters: seasonal, annual and diurnal. It is important to realize that it is not the total amount of rain which falls during a given year that matters, but rather the period of time for which the rainfall rate exceeds a certain value. All of these temporal variations were estimated by use of (28) for rain attenuation, which does not exceed 0.01 % of the time. Thus, according to [3]:

$$L_{0.01} = a(f)R_{0.01}^{b(f)s_{0.01}R}, \quad (28)$$

where $s_{0.01}$ can be found in [3]. For time percentages other than 0.01 %, the attenuation can be corrected by introducing special relevant time percentage P, which is changed over the wide range from 0.001 to 1 % [3], that is:

$$L(P) = L_{0.01} \times 0.12P^{-(0.546 + 0.043\log P)}. \quad (29)$$

The precipitation of rain is defined by variations in both horizontal and vertical directions that make in very hard to describe the spatial distribution of rain. The correction factor we use in (28) is the effective path length [the exponent $s_{0.01}r_R$ in (28)], L_r, which is the length of the hypothetical path obtained from signal data, dividing the total attenuation by the specific attenuation exceeded for the same percentage of time [3]. It can be estimated, according to empirical model [15] as

$$L_r = \frac{L_s}{1 + 0.0286L_h R^{0.15}}. \quad (30)$$

Using equations (27) and (30) we can now estimate that the transmission loss due to attenuation by rain is given by

$$A_r = \gamma_r L_r. \quad (31)$$

Effects of clouds

As was mentioned earlier, the dimension, shape, structure and texture of clouds are influenced by air movements that change their formation and growth, and by the properties of the cloud particles. Sky cover is the observer view of the cover of the sky dome, whereas cloud cover can be used to describe areas that are smaller or larger than the floor space of the sky dome [2]. There are several proposed models for the probability distribution of the sky cover [11–13]. For our prediction of the cloud attenuation, we will use the ITU-R model given in [11].

Specific attenuation for clouds. The specific attenuation due to a cloud can be determined by [2]

$$\gamma_c = K_1 M \left[\frac{\mathrm{dB}}{\mathrm{km}}\right], \quad (32)$$

where γ_c is the specific attenuation of the clouds, dB/km; K_1 is the specific attenuation coefficient, (dB/km)/(g/m^{-3}); M is liquid water density, g/m^{-3}.

For small size cloud droplets, the *Rayleigh approximation* can be used for the calculation of specific attenuation [2]. This approximation is valid up to 100 GHz. A mathematical model based on Rayleigh scattering, which uses a double-Debye model for the dielectric permittivity $\varepsilon(f)$ of water, can be used to calculate the value of K_1:

$$K_1 = \frac{0.8197f}{\varepsilon''\left(1+\eta^2\right)}\left[\frac{\text{dB}}{\text{km}}\right]\left[\frac{\text{g}}{\text{m}^{-3}}\right]^{-1}, \qquad (33)$$

where f is the frequency, GHz, and η defined as

$$\eta = \frac{2+\varepsilon'}{\varepsilon''}, \qquad (34)$$

where ε' and ε'' are the real and imaginary components of the complex dielectric permittivity of water. For the calculation of the complex dielectric permittivity of water, we need to calculate the principle and secondary frequencies of the double Debye model for the dielectric permittivity of water:

$$f_p = 20.09 - 142(\Phi - 1) + 294(\Phi - 1)^2; \qquad (35a)$$

$$f_s = 590 - 1500(\Phi - 1), \qquad (35b)$$

where $\Phi = 300/T$, T is the temperature, K. Now we can define the complex dielectric permittivity of water as

$$\varepsilon'(f) = \frac{(\varepsilon_0 - \varepsilon_1)}{1+\left(\frac{f}{f_p}\right)^2} + \frac{(\varepsilon_1 - \varepsilon_2)}{1+\left(\frac{f}{f_s}\right)^2} + \varepsilon_2; \qquad (36)$$

$$\varepsilon''(f) = \frac{f(\varepsilon_0 - \varepsilon_1)}{f_p\left(1+\left(\frac{f}{f_p}\right)^2\right)} + \frac{f(\varepsilon_1 - \varepsilon_2)}{f_s\left(1+\left(\frac{f}{f_s}\right)^2\right)}, \qquad (37)$$

where $\varepsilon_0 = 77.6 + 103.3(\Phi - 1)$; $\varepsilon_1 = 5.48$; $\varepsilon_2 = 3.51$.

Figure 5, computed by using the above formulas, shows the values of the specific attenuation K_1 at frequencies from 1 to 5 GHz and temperatures between –8 and 20 °C.

Total cloud attenuation. Finally, we can determine the total cloud attenuation:

$$A = \frac{LK_1}{\sin(\theta)}, \qquad (38)$$

where L is the total columnar content of liquid water, kg/m^2, or, equivalently, in millimeters of evaporated water; K_1 is the specific attenuation coefficient as described earlier in (33), (dB/km)/(g/m^{-3}); θ is the elevation angle ($5° \le \theta \le 90°$).

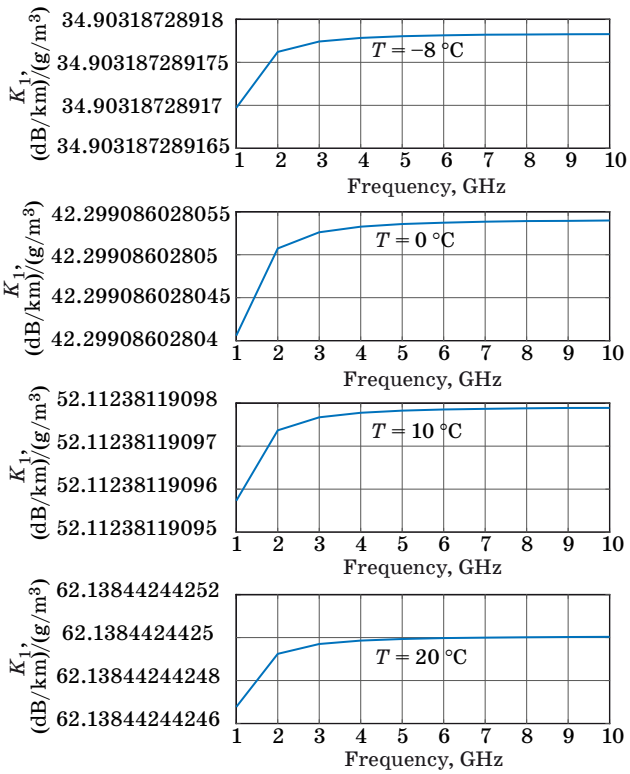

■ ***Fig. 5.*** Specific attenuation for clouds as a function of frequency and temperature

Figure 6 shows total cloud attenuation as a function of frequency, for elevation angles from 3 to 29° [11]. Our computations are based on liquid water content of 0.29 kg/m^3.

Effects of turbulence

Atmospheric turbulence is a chaotic phenomenon created by the random temperature, wind magnitude variation, and direction variation in the propagation [4]. This chaotic behavior resulting in index-of-refraction fluctuations, causes Doppler shift and fast fading phenomena. As is common for describing atmospheric turbulence, we use Turbulence Power Spectra that are divided into three regions by two scale sizes: L_0 — the outer scale of the turbulence varies between 10 to 100 m and l_0 — the inner scale typically observed from 1 to 30 mm. The regions that are divided by those scales are called *scintillations* in the literature [4–7].

Scintillation index. The scintillation index (normalized variance of signal intensity fluctuations) σ_I^2 describes fluctuations in optical power as measured by a point detector. The scintillation index is defined by [4–7]

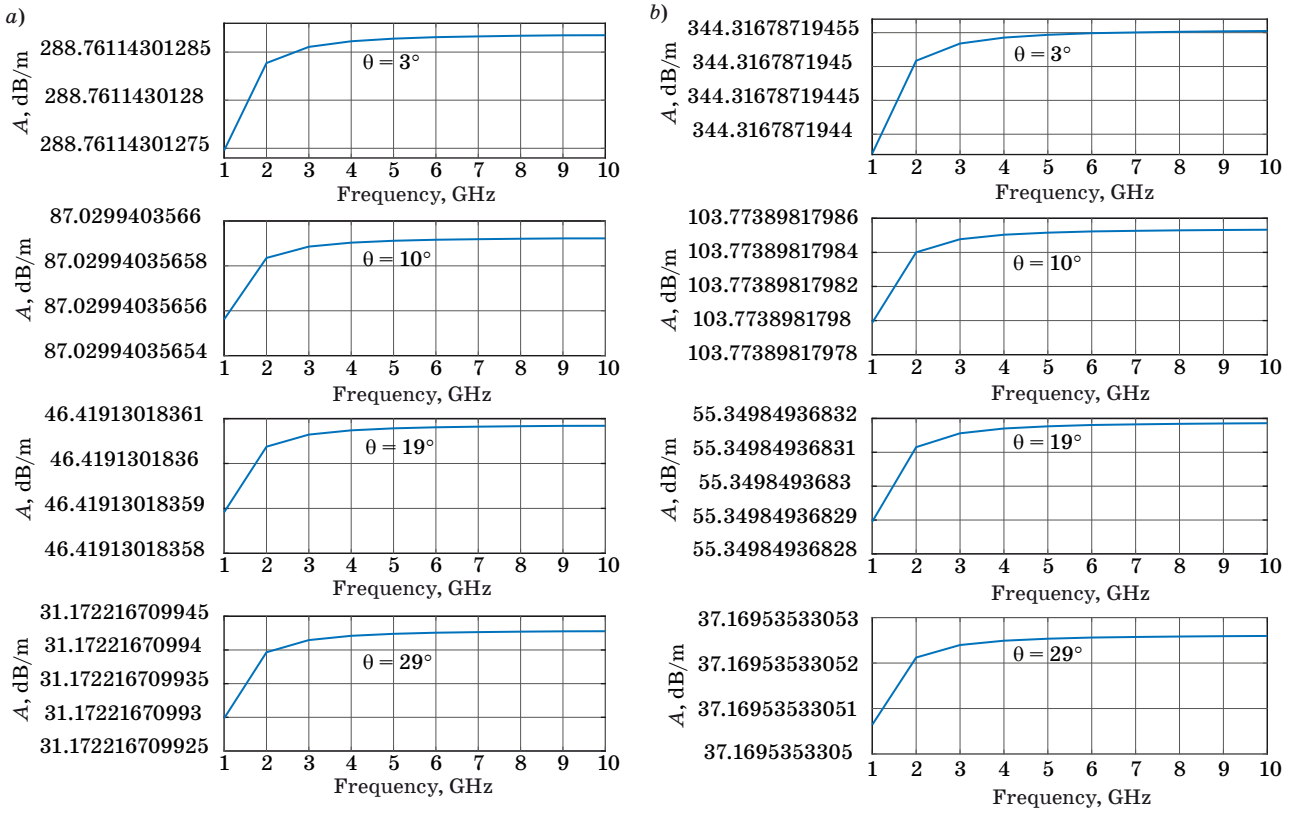

■ ***Fig. 6.*** Total cloud attenuation as a function of frequency, for elevation angles from 3 to 29°: *a* — $T = 10$ °C; *b* — $T = 20$ °C

$$\sigma_I^2 = \frac{\langle I^2 \rangle - \langle I \rangle^2}{\langle I \rangle^2} = \frac{\langle I^2 \rangle}{\langle I \rangle^2} - 1. \qquad (39)$$

It relates to the Rytov variance (log-amplitude variance) σ_R^2 according to [4–7]. According to [23] the Rytov, approximation starts from the premise that an air mass behaves as a fluid. Assuming that the refractive index structure parameter is constant, the basic Rytov approximation relative variance is [6, 23]:

$$\sigma_R^2 = 1.23 \cdot C_n^2 \cdot k^{7/6} \cdot L^{11/6}, \qquad (40)$$

where C_n^2 is the refractive index structure parameter; k is the wave number, $k = 2\pi/\lambda$; L is the distance, km. Figure 7 illustrates behavior of the Rytov's scintillation index vs. distance between the terminals L for various f and refraction structure parameters C_n^2.

As can be seen from Figs. 7, *a*–*c*, much stronger turbulence (with increase of C_n^2) in the atmosphere, leads to higher deviations of signal intensity variations — the effect increases non-linearly with an increase of range between the source and the detector. This increase effect is also clearly seen from results of computations presented in Fig. 8, where the same Rytov's scintillation index is presented as a function of C_n^2 for three frequencies, $f = 2.5$, 3.3, and 5.2 GHz, that are usually used in land-atmospheric communication networks (namely, in Wi-Fi wireless communication).

As can be seen from Fig. 8, with the increasing of frequencies, the Rytov's scintillation index increases linearly as a function of C_n^2. Consequently, the fading effect becomes significant for signals passed over the turbulent atmospheric channel. Moreover, with an increase of frequency from 2.4 to 5.2 GHz, the scintillation index increases roughly twice thus causing strong fading of signals passing through a turbulent tropospheric channel.

It was shown experimentally [6, 7, 23] that the signal intensity scintillations, caused by quasi-local atmospheric turbulence, are distributed log-normally. In this case, it can be suggested that the fluctuations of the radio or optical signals are weak. The normalized standard deviation of this distribution is proportional to the Rytov's approximation and can be written now via the structure parameter of turbulence permittivity C_ε^2 (instead of the structure parameter of refractivity C_n^2) as [6, 7, 23]

$$\sigma_I^2 = 0.12 \cdot C_\varepsilon^2 \cdot k^{7/6} \cdot L^{11/6}. \qquad (41)$$

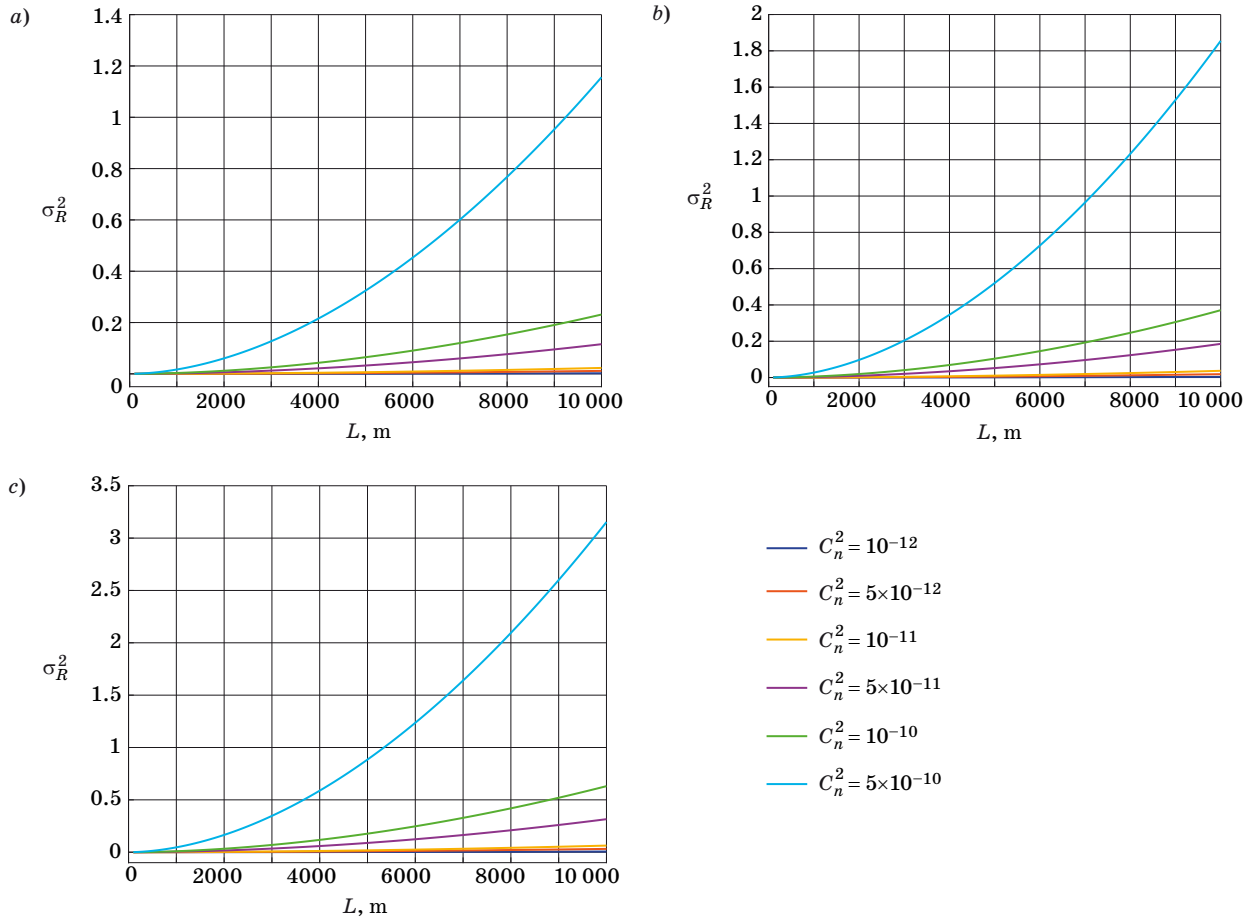

■ ***Fig. 7***. Rytov's scintillation index vs. distance between the terminals L for various refraction structure parameters of the turbulent atmosphere C_n^2 : *a* — $f = 2.4$ GHz; *b* — $f = 3.3$ GHz; *c* — $f = 5.2$ GHz

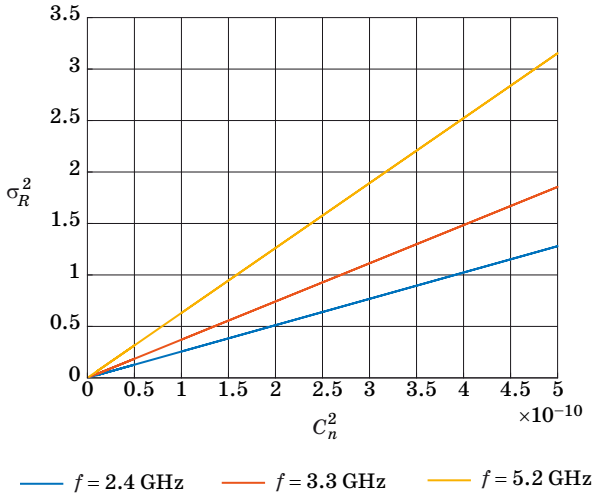

■ ***Fig. 8***. Rytov's scintillation index vs. C_n^2 for different frequencies f

We should note that C_ε^2 is the structure constant of the turbulence permittivity averaged over the path L [km], k is the wave number mentioned above.

In Fig. 9 we present the computed index of signal intensity scintillations versus the structure constant of the turbulence averaged over the path for different frequencies from 1 to 50 GHz.

It can be seen that approximately for $C_\varepsilon^2 = 10^{-10}$ the signal immediately starts to deteriorate; and as the frequency increases, the index of signal intensity scintillations becomes twice as strong. This result is very important for us because it helps us predict the fast fading of the signal within land aircraft radio communication links passing through the turbulent troposphere and operating at frequencies in the L/X-band ($f > 1...10$ GHz).

The fast fading of the signal at open paths is caused mainly by multipath propagation and turbulent fluctuations of the refractive index. The fluctuations of the signal intensity due to turbulence are distributed log-normally with the normalized standard deviation described by the Rytov variance. For weak fluctuation with the Rytov method, the scintillation index can be expressed in the following form:

$$\sigma_I^2 = \exp\left(4\sigma_R^2\right) - 1. \qquad (42)$$

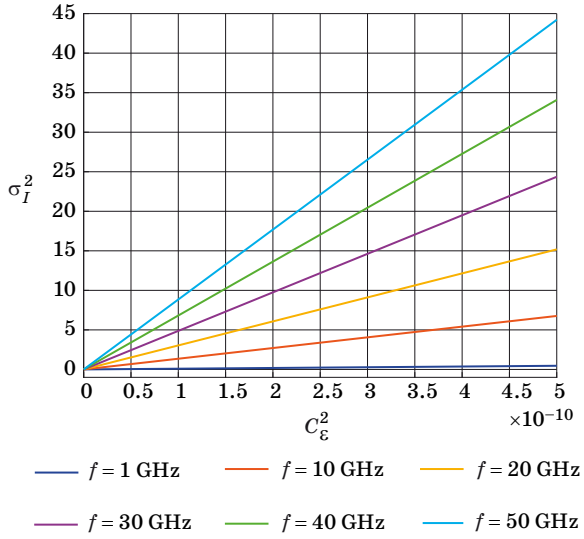

■ ***Fig. 9.*** Index of signal intensity scintillations versus the structure constant of the turbulence averaged over the path for frequencies from 1 to 50 GHz for L = 10 km

The turbulence attenuation related to scintillation is equal to σ_R^2 [dB] and thus the relation for turbulence attenuation γ_R according to Rytov's theory of regular turbulence can be written as [6, 7]

$$\gamma_R = 2\sqrt{23.17 \cdot C_\varepsilon^2 \cdot k^{7/6} \cdot L^{11/6}}. \qquad (43)$$

Relation of scintillation index and K-parameter of fast fading. Another way to calculate the attenuation due to fast fading effects is to use the relations between K and the scintillation index σ_I. Usually in land wireless communication, instead of σ_I^2 parameter of fading K is used [4, 5]. For Gaussian distribution described zero-mean random process of turbulent structures evolution (usually observed experimentally in the irregular atmosphere), we could define the relation between the Ricean parameter of fading K, introduced above, and the scintillation index σ_I as

$$\left\langle \sigma_I^2 \right\rangle = \frac{\left\langle \left[I - \langle I \rangle \right]^2 \right\rangle}{\langle I \rangle^2} = \frac{I_{inc}^2}{I_{co}^2} \equiv K^{-2}, \qquad (44)$$

where I_{co} and I_{inc} are the coherent and incoherent components of the total signal intensity. Results of computations according to (44) are shown in Fig. 10.

The range $\left\langle \sigma_I^2 \right\rangle$ of the scintillation index variations, from 0.2 to 0.8, was obtained from numerous experiments, where relations between this parameter and the refractivity of the turbulence in the irregular atmosphere were taken into account [4–7, 25, 26]. Thus, from experiments described

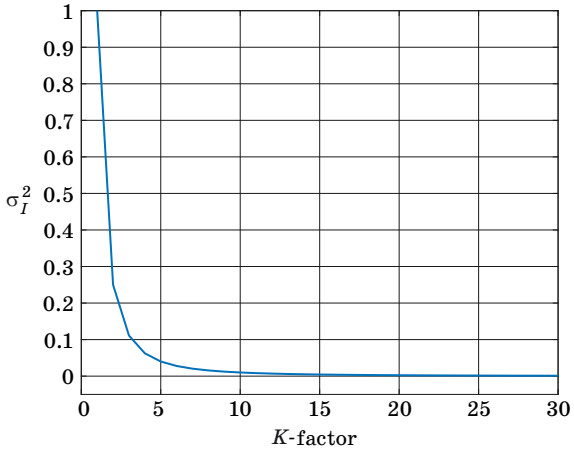

■ ***Fig. 10.*** Scintillation index vs. Ricean fading parameter K

there, it was estimated: $\sim C_n^2 \approx 10^{-15}\,\mathrm{m}^{-2/3}$ and $\sim C_n^2 \approx 10^{-13}\,m^{-2/3}$, for a nocturnal and a diurnal atmosphere at the height around 1–2 km, respectively. As follows from (44), for $\left\langle \sigma_I^2 \right\rangle$ changing from 0.2 to 0.8, the fading parameter K changes from ~1.2–1.3 to ~3.5–3.8. This indicates the existence of direct visibility between both terminals, the source and the detector, accompanied by the weak additional effects of multipath phenomena caused by multiple scattering of signals at the turbulent structures, formed in the disturbed atmospheric regions, observed experimentally [5, 7, 25, 26]. In other words, a non-linear relation between K and σ_I^2 states: when K is high the scintillation index is low and vice versa; when σ_I^2 grows to its maximum value, parameter K reduces to its minimum value. When this occurs, we get the worst Rayleigh distribution and the biggest attenuation. The K-parameter can be used to determine the capacity, spectral efficiency, and BER of data stream sent via communication channel.

To be continued.

References

1. Zuev V. E., and G. M. Krekov. *Optical Methods in the Atmosphere*. Leningrad, Gidrometeoizdat Publ., 1986.
2. Kopeika N. S. *A System Engineering Approach to Imaging*, Billingham, WA, SPIE Press, 1998. 704 p.
3. Saunders S. R. *Antennas and Propagation for Wireless Communication Systems*. John Wiley & Sons, New York, 2007. 546 p.
4. Blaunstei N., and Ch. Christodoulou. *Radio Propagation and Adaptive Antennas for Wireless Communication Links: Terrestrial, Atmospheric and Ionospheric*. Wiley InterScience, NJ, 2007. 614 p.

5. Blaunstein N., and Ch. Christodoulou. *Radio Propagation and Adaptive Antennas for Wireless Communication Networks: Terrestrial, Atmospheric and Ionospheric*, Wiley, NJ, 2014. 704 p.
6. Blaunstein N., Arnon Sh., Zilberman A., and Kopeika N. *Applied Aspects of Optical Communication and LIDAR*. New York, CRC Press, Taylor &Francis Group, 2010. 262 p.
7. *Optical Waves and Laser Beams in the Irregular Atmosphere*. Ed. by N. Blaunstein, and N. Kopeika. Boca Raton, FL, CRC Press, Taylor&Frances Group, 2018. 334 p,
8. d'Almeida G. A., Koepke P., Shettle E. P. *Atmospheric Aerosols. Global Climatology and Radiative Characteristics*. Deepak Publishing, Hampton, 1991. 561 p.
9. Deirmendjian D. *Electromagnetic Scattering on Spherical Polydispersions*. American Elsevier, New York, 1969. 318 p.
10. Seinfeld J. H. *Atmospheric Chemistry and Physics of Air Pollution*. John Wiley & Sons, New York, 1986. 768 p.
11. Attenuation due to clouds and fog. *ITU-R Recommendation International Telecommunication Union*, 1992, pp. 840–842.
12. Chou M. D. Parametrizations for cloud overlapping and shortwave single scattering properties for use in general circulation and cloud ensemble models. *J. Climate*, 1998, vol. 11, pp. 202–214.
13. Wei Zhang. Scattering of radiowaves by a melting layer of precipitation in backward and forward directions. *IEEE Transactions on Antennas and Propagation*, 1994, vol. 42, no. 3, pp. 347–356.
14. Crane R. K. Prediction of attenuation by rain. *IEEE Trans. Commun*, 1980, vol. 28, pp. 1717–1733.
15. Lin D. P., and Chen H. Y. An empirical formula for the prediction of rain attenuation in frequency range 0.6–100 GHz. *IEEE Trans. on Antennas Propagat*, 2002, vol. 50, pp. 545–551.
16. *ITU-R Recommendation International Telecommunication Union "Specific attenuation model for rain for use in prediction methods"*, Geneva, 1992, p. 838.
17. Kooi P.-S., Leong M.-S., Li L.-W., et al. Microwave attenuation by realistically distorted raindrops: Part II — predictions. *IEEE Transactions on Antennas and Propagation*, 1995, vol. 43, pp. 821–828.
18. Jaenicke R. *Aerosol Physics and Chemistry*. In: *Physical Chemical Properties of the Air, Geophysics and Space Research*, vol. 4 (b). Ed. G. Fisher. Berlin, Springer-Verlag, 1988.
19. Rosen J. M., and Hofmann D. J. Optical modeling of stratospheric aerosols: present status. *Appl. Opt.*, 1986, vol. 25(3), pp. 410–419.
20. *ITU-R International Telecommunication Union, ITU-R Recommendation "Attenuation by atmospheric gases"*, 1997, pp. 676–683.
21. *ITU-R Recommendation International Telecommunication Union "Propagation data and prediction methods required for the design of terrestrial line-of-sight systems"*, 1997, pp. 530–537.
22. *ITU-R Recommendation International Telecommunication Union "Characteristics of precipitation for propagating modeling"*, 1992, p. 837.
23. Ishimaru A. *Wave Propagation and Scattering in Random Media*. Academic Press, New York, 1978. 272 p.
24. Andrews L. C., and Phillips R. L. *Laser Beam Propagation through Random Media*. 2nd Ed. SPIE Press, Bellingham, WA, USA, 2005. 808 p.
25. Bendersky S., Kopeika N., and Blaustein N. Prediction and modeling of line-of-sight bending near ground level for long atmospheric paths. *Proc. of SPIE Int. Conf.*, San Dieg, August 3–8, 2004, pp. 512–522.
26. Bendersky S., Kopeika N., and Blaunstein N. Atmospheric optical turbulence over land in middle-east coastal environments: prediction, modeling and measurements. *J. Applied Optics*, 2004, vol. 43, pp. 4070–4079.